

AD-A266 243



PL-TR-92-2343

DTIC
ELECTE
JUN 23 1993
S C D

2

POLAR 2 MODEL OF THE WAKE SHIELD EXPERIMENT

M. F. Tautz

Radex, Inc.
Three Preston Court
Bedford, MA 01730

December 16, 1992

Scientific Report No. 12

Reproduced From
Best Available Copy

Approved for public release; distribution unlimited

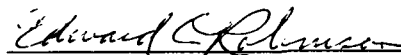
93 6 22-020

93-14040



PHILLIPS LABORATORY
Directorate of Geophysics
AIR FORCE MATERIEL COMMAND
HANSCOM AIR FORCE BASE, MA 01731-5000

"This technical report has been reviewed and is approved for publication"



EDWARD C. ROBINSON
Contract Manager
Data Analysis Division



ROBERT E. MCINERNEY, Director
Data Analysis Division

This report has been reviewed by the ESD Public Affairs Office (PA) and is releasable to the National Technical Information Service (NTIS).

Qualified requestors may obtain additional copies from the Defense Technical Information Center. All others should apply to the National Technical Information Service.

If your address has changed, or if you wish to be removed from the mailing list, or if the addressee is no longer employed by your organization, please notify GL/IMA, Hanscom AFB, MA 01731. This will assist us in maintaining a current mailing list.

Do not return copies of this report unless contractual obligations or notices on a specific document requires that it be returned.

REPORT DOCUMENTATION PAGE			Form Approved OMB No. 0704-0188	
<small>Public reporting burden for this collection of information is estimated to average 1 hour per response, including the time for reviewing instructions, searching existing data sources, gathering and maintaining the data needed, and completing and reviewing the collection of information. Send comments regarding this burden estimate or any other aspect of this collection of information, including suggestions for reducing this burden, to Washington Headquarters Services, Directorate for Information Operations and Reports, 1215 Jefferson Davis Highway, Suite 1204, Arlington, VA 22202-4302, and to the Office of Management and Budget, Paperwork Reduction Project (0704-0188), Washington, DC 20503.</small>				
1. AGENCY USE ONLY (Leave blank)	2. REPORT DATE 16 December 1992	3. REPORT TYPE AND DATES COVERED Scientific Report No. 12		
4. TITLE AND SUBTITLE POLAR 2 Model of the Wake Shield Experiment		5. FUNDING NUMBERS PE 62101F PR 7659 TA 05 WU AB Contract F19628-89-C-0068		
6. AUTHOR(S) M. F. Tautz		8. PERFORMING ORGANIZATION REPORT NUMBER RXR-92121		
7. PERFORMING ORGANIZATION NAME(S) AND ADDRESS(ES) RADEX, Inc. Three Preston Court Bedford, MA 01730		10. SPONSORING MONITORING AGENCY REPORT NUMBER PL-TR-92-2343		
9. SPONSORING MONITORING AGENCY NAME(S) AND ADDRESS(ES) Phillips Laboratory Hanscom AFB, MA 01731-5000 Contract Manager: Edward C. Robinson/GPD		11. SUPPLEMENTARY NOTES		
12a. DISTRIBUTION AVAILABILITY STATEMENT Approved for Public Release Distribution Unlimited		12b. DISTRIBUTION CODE		
13. ABSTRACT (Maximum 200 words) The current-voltage characteristic of a charged probe in the wake of a shielding disk is calculated using the POLAR code. The current-voltage curves are parameterized with respect to the tilt angle of the shielding disk. Estimates of the magnitude of probe current for conditions simulating the CHAWS space shuttle experiment are given.				
14. SUBJECT TERMS Plasma, POLAR code, computer simulation, CHAWS experiment, IV characteristic			15. NUMBER OF PAGES 46	
			16. PRICE CODE	
17. SECURITY CLASSIFICATION OF REPORT Unclassified	18. SECURITY CLASSIFICATION OF THIS PAGE Unclassified	19. SECURITY CLASSIFICATION OF ABSTRACT Unclassified	20. LIMITATION OF ABSTRACT Unlimited	

NSA 7540-01-30-5500

Standard Form 298, Rev. 1-89
Prescribed by ANSI Z39-18, 1983

TABLE OF CONTENTS

<u>Section</u>	<u>Page</u>
1.0 INTRODUCTION	1
2.0 CALCULATION SCHEME FOR THE POLAR 2 MODEL	3
3.0 POLAR 2 RESULTS FOR THE WAKE SHIELD MODEL	10
4.0 CONCLUSIONS	36
REFERENCES	37
APPENDIX. POLAR 2 PROGRAMMING NOTES	39

Accession For	
NTIS CRA&I	<input checked="" type="checkbox"/>
DTIC TAB	<input type="checkbox"/>
Unannounced	<input type="checkbox"/>
Justification	
By	
Distribution /	
Availability Codes	
Dist	Avail and/or Special
A-1	

List of Figures

<u>Figure</u>	<u>Page</u>
1. Schematic of Wake Shield Model	2
2. Schematic of POLAR 2 Setup Configuration	4
3. POLAR 1 model of shielding disk	5
4. POLAR 1 model of shielded probe	6
5(a). POLAR 2 model of disk and probe, top view	7
5(b). POLAR 2 model of disk and probe, side view	8
5(c). POLAR 2 model of disk and probe, back view	9
6(a). POLAR 1 geometrical ions, tilt = 0 degrees	11
6(b). POLAR 1 geometrical ions, tilt = +20 degrees	12
6(c). POLAR 1 geometrical ions, tilt = +40 degrees	13
7(a). POLAR 2 potential contours; probe at -1kV, D = 0.35, tilt = +40 degrees	14
7(b). POLAR 2 potential contours; probe at -1kV, D = 0.35, tilt = +20 degrees	15
7(c). POLAR 2 potential contours; probe at -1kV, D = 0.35, tilt = 0 degrees	16
7(d). POLAR 2 potential contours; probe at -1kV, D = 0.35, tilt = -20 degrees	17
7(e). POLAR 2 potential contours; probe at -1kV, D = 0.35, tilt = -40 degrees	18
7(f). POLAR 2 potential contours; probe at -9kV, D = 0.35, tilt = +40 degrees	19
7(g). POLAR 2 potential contours; probe at -9kV, D = 0.35, tilt = +20 degrees	20
7(h). POLAR 2 potential contours; probe at -9kV, D = 0.35, tilt = 0 degrees	21
7(i). POLAR 2 potential contours; probe at -9kV, D = 0.35, tilt = -20 degrees	22
7(j). POLAR 2 potential contours; probe at -9kV, D = 0.35, tilt = -40 degrees	23
8. Current-Voltage characteristics for D = 0.35	24
9. Probe currents versus tilt, D = 0.35	25
10. POLAR 2 trajectories, D = 0.35	27
11(a). POLAR 2 potential contours; probe at -9kV, D = 1.05, tilt = +40 degrees	28
11(b). POLAR 2 potential contours; probe at -9kV, D = 1.05, tilt = 0 degrees	29
11(c). POLAR 2 potential contours; probe at -9kV, D = 1.05, tilt = -40 degrees	30
12. Current-Voltage characteristics for D = 1.05	31
13. Probe currents versus tilt, D = 1.05	32
14. Surface cell numbers on the probe	33
15. Surface cell currents, D = 0.35	34
16. Surface cell currents, D = 1.05	35

List of Tables

<u>Table</u>	<u>Page</u>
1. Wake Shield Model Input Parameters	1

ACKNOWLEDGEMENTS

The author wishes to thank Dr. David L. Cooke for his help and guidance with the POLAR code, and in interpreting the physics results. The approach taken here was suggested by Dr. Cooke, and his help was invaluable in diagnosing and debugging the POLAR 2 code runs.

1.0 INTRODUCTION

The proposed wake shield experiment will study the current-voltage (IV) characteristic of a charged probe mounted on an uncharged shielding disk, which will be oriented through a sequence of tilt angles with respect to the shuttle direction of motion. In this report, we summarize calculations done with the POLAR 2 code to model the IV characteristic of the wake-shield probe for typical orbit environments.

The normal version (POLAR 1) of the POLAR code [Lilley, *et al.*, 1989] has been used extensively to study charging effects in space [Cooke, *et al.*, 1989] and in vacuum chambers [Chan, *et al.*, 1993]. The POLAR 2 code [Jongeward, *et al.*, 1988], on the other hand, is an experimental version of POLAR which has gone through a very limited validation phase. POLAR 2 was written by S-Cubed to analyze the plasma sheath and current collection in the SPEAR I rocket experiment [Katz, *et al.*, 1989]. It contains the same physical models as POLAR 1 (although several features are not fully implemented) and allows for multiple grids. The multi-grid capability is required for problems with large computational spaces and localized high resolution regions, such as SPEAR I. In the wake-shield experiment, the probe dimensions are small compared to those of the shielding disk, and in order to do the simulations efficiently and with adequate resolution, we have used the multi-grid feature of POLAR 2. Thus, we have employed two grids in our wake-shield model: a course grid to represent the exterior plasma region and the shielding disk, and a nested fine grid to resolve the region surrounding the charged probe.

In this study, we have taken as the nominal configuration the case where the front disk is oriented perpendicular to the flow direction. We then consider tilt angles to plus and minus 40 degrees away from the nominal orientation, as depicted in Figure 1. The main objective of this investigation was to calculate the IV curve for the probe as a function of the tilt angle. A list of all the physics input parameters that were used is given in Table 1. Note that the probe size is very much smaller than the disk dimensions (ratio of 30:1), and that to properly resolve the experiment in the probe region, we were driven to employ a multi-grid representation of the problem.

TABLE 1. Wake Shield Model Input Parameters

Parameter	Value
Diameter of shielding disk	3.0 M
Width of probe	8.33 cm
Length of probe	25.0 cm
Plasma ambient temperature	0.2 eV
Plasma ambient density	9×10^{11} , 1×10^{11} #/M ³
Plasma ambient Debye length	0.35, 1.05 cm
Ion mass	16.0 AMU
Plasma acoustic velocity (vt)	1.1 km/sec
Shuttle velocity (vs)	7.68 km/sec
Ion Mach number (vs/vt)	7.0
Tilt angles	-40, -20, 0, 20, 40 degrees
Probe voltages	-1, -3, -5, -7, -9 kV

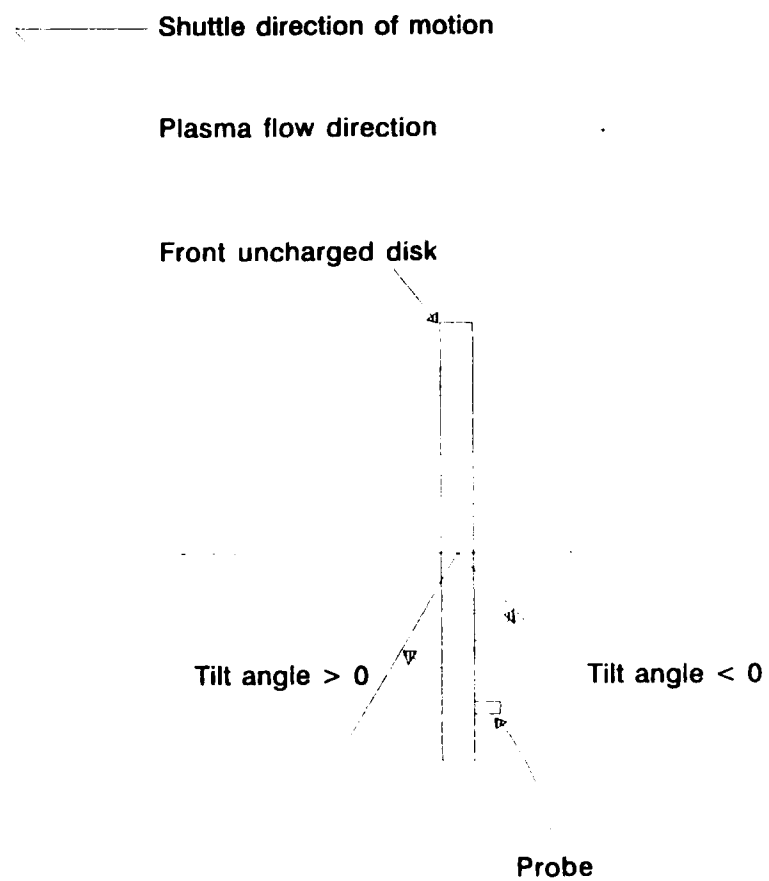


Figure 1. Schematic of Wake Shield Model.

In section 2, we describe the POLAR 2 multi-grid model of the wake shield experiment, and section 3 summarizes the physics results obtained from the simulations. The last section contains the conclusions to be reached from this study.

POLAR 2 is an unfinished, experimental version of POLAR and, as such, required a considerable programming effort to enable it to produce reliable physics output. Some of the special programming considerations that were needed to implement POLAR 2 are contained in the Appendix.

2.0 CALCULATION SCHEME FOR THE POLAR 2 MODEL

Figure 2 shows a schematic of the sequence of run submissions used for setting up each POLAR 2 case. In the Figure, the box on the lower right represents the run that actually generates the IV characteristic for a given tilt angle. The other boxes represent tasks that were needed to prepare the tilt angle geometry. Each box indicates briefly the task to be performed, and the arrows indicate the dependency paths. A fuller explanation is given below.

The POLAR 2 code does not have a vehicle module for building objects. Instead, it has the PATCHV program which enables one to take POLAR 1 objects and combine them into a multi-grid representation for POLAR 2. To orient the probe, a grid scaling factor and the position of the nested inner grids with respect to the outer grid is set in PATCHV. To specify the wake shield problem, we have built a POLAR 1 model of the front disk and taken this as the outer grid. A POLAR 1 model of the probe was also constructed, and this was specified to be an inner grid. The two grids were then combined by means of PATCHV to form the resultant POLAR 2 computational space.

Figure 3 shows the POLAR 1 model of the front disk. It is an octagon made of conducting material (the type of material does not matter since the surface potential was held constant) of width 9 grid units and side 5. The disk was chosen to be of minimum thickness, which is one grid unit. Physical dimensions of meters were specified by setting each mesh unit cube to have sides of length 0.33 meters, which corresponds to a 3 meter diameter disk.

Figure 4 shows the POLAR 1 representation of the probe. It is made up of 3 conducting cubes stacked along the z direction. The back plate was added to facilitate connection to the disk. This model has $3 \times 4 \times 1 = 12$ outward faces, each of which can be monitored separately for current collection.

Figure 5 shows the multi-grid object obtained by combining the above disk and probe models. The probe inner grid was taken to be smaller than the outer grid by a 4:1 ratio. This means that physically the probe cubes are of side $0.333/4 = 0.0833$ Meters. The probe was positioned off center in the negative x direction. The distance from the probe center to the nearest disk edge is ~ 5.5 inner mesh units, or 0.42 Meters.

The POLAR 2 code does not calculate the geometrical ion (GI) density. This neutral density is needed to represent ions in the region outside the sheath where particle tracking is not done. Thus, in order to proceed, there were two options considered:

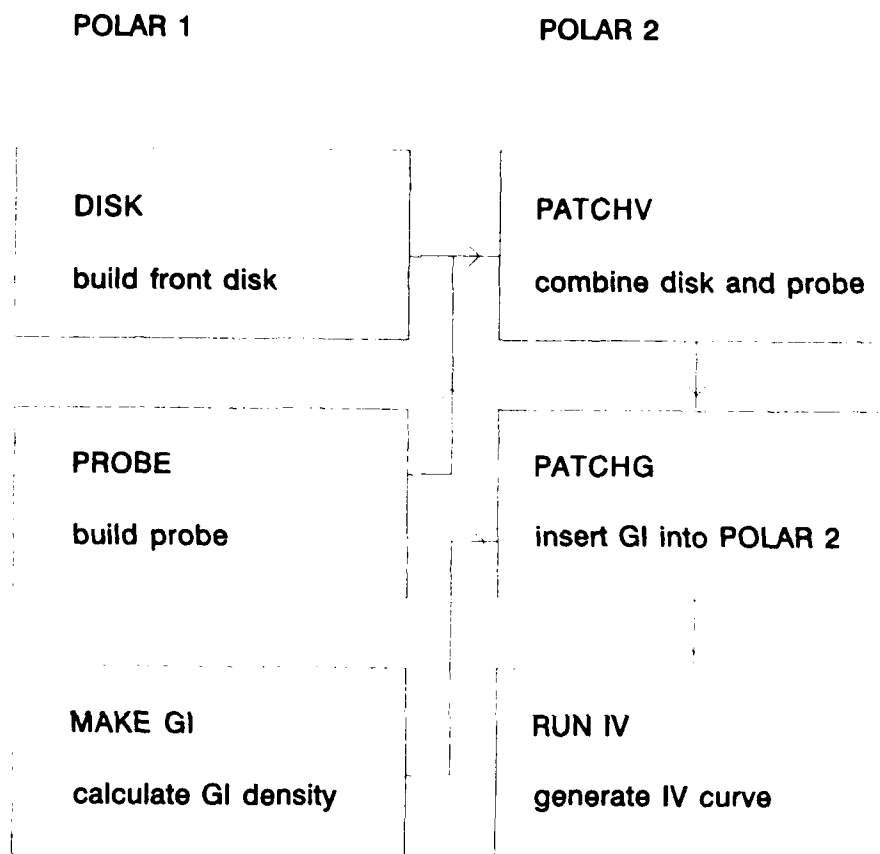
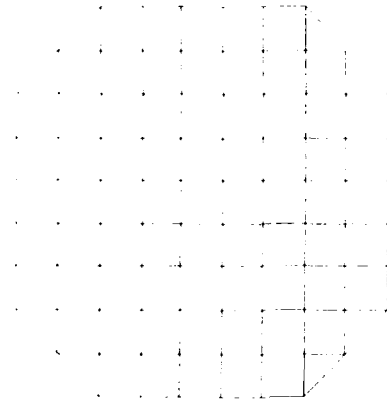


Figure 2. Schematic of POLAR 2 Setup Configuration.

material legend SURFACE CELL MATERIAL COMPOSITION AS VIEWED FROM
 THE POSITIVE Z DIRECTION FOR Z VALUES BETWEEN 1 AND 33

1
 SILV

17.
 16.
 15.
 14.
 13.
 12.
 11.
 10.
 9.
 8.
 7.
 6.
 5.
 4.
 3.
 2.
 1.



Y

1. 2. 3. 4. 5. 6. 7. 8. 9. 10. 11. 12. 13. 14. 15. 16. 17.

— X —

Figure 3. POLAR 1 model of shielding disk.

SURFACE CELL MATERIAL COMPOSITION AS VIEWED
FROM THE NEGATIVE X DIRECTION FOR X VALUES
BETWEEN 1 AND 17

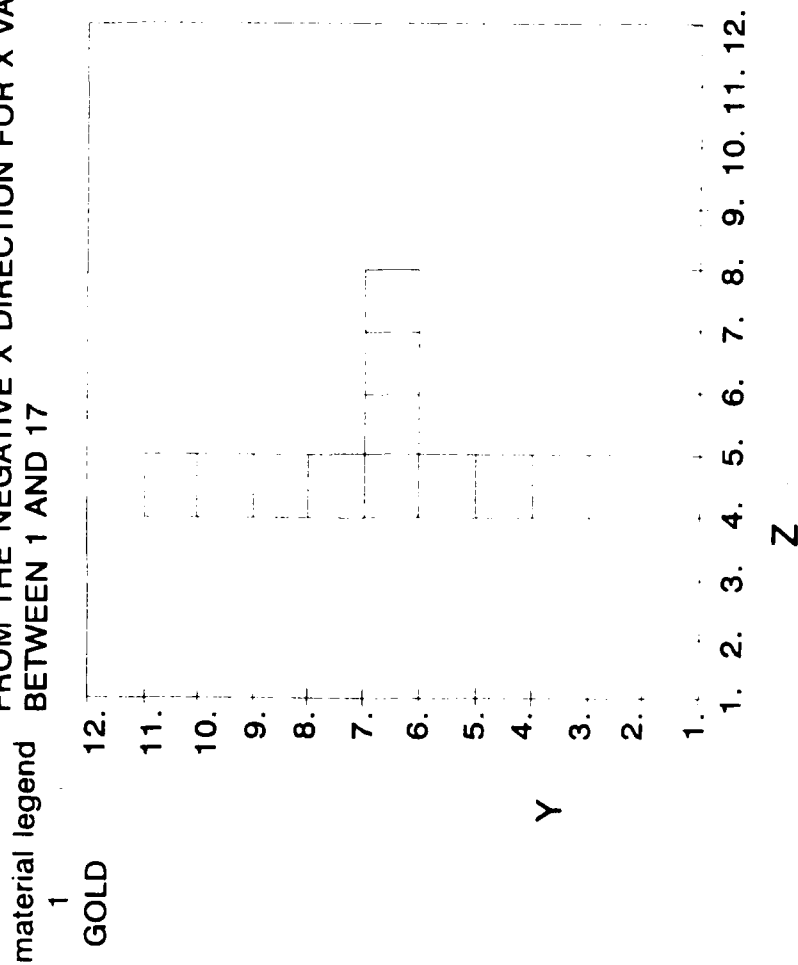


Figure 4. POLAR 1 model of shielded probe.

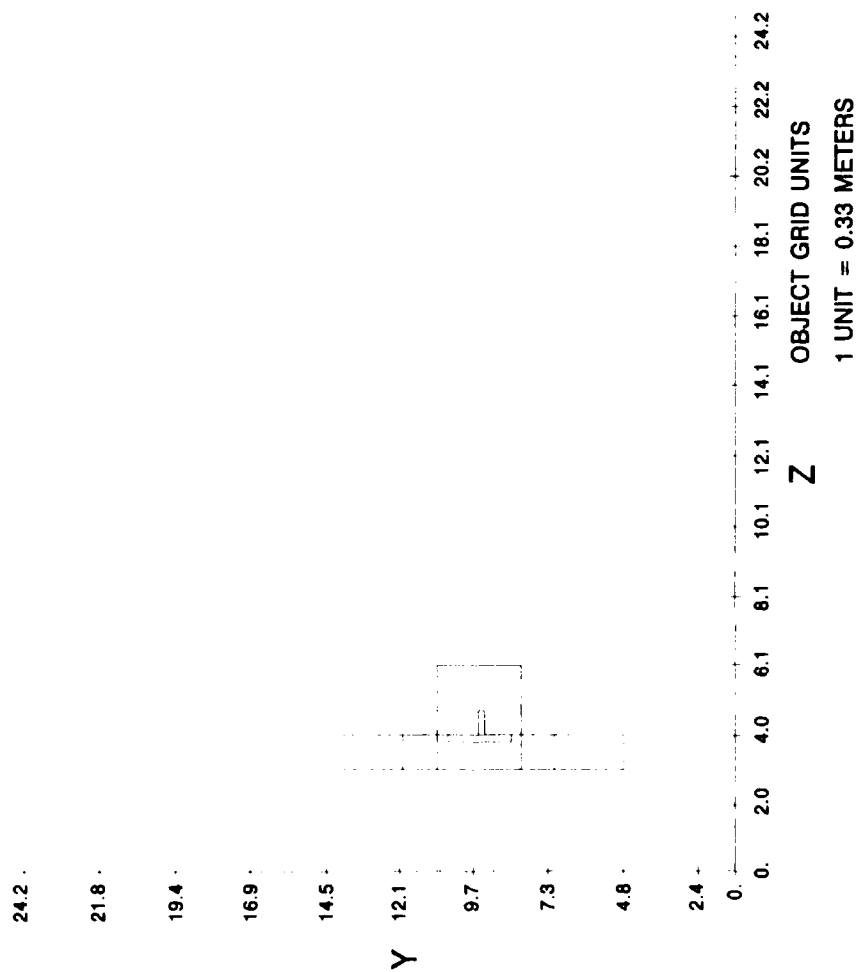


Figure 5(a). POLAR 2 model of disk and probe, top view.

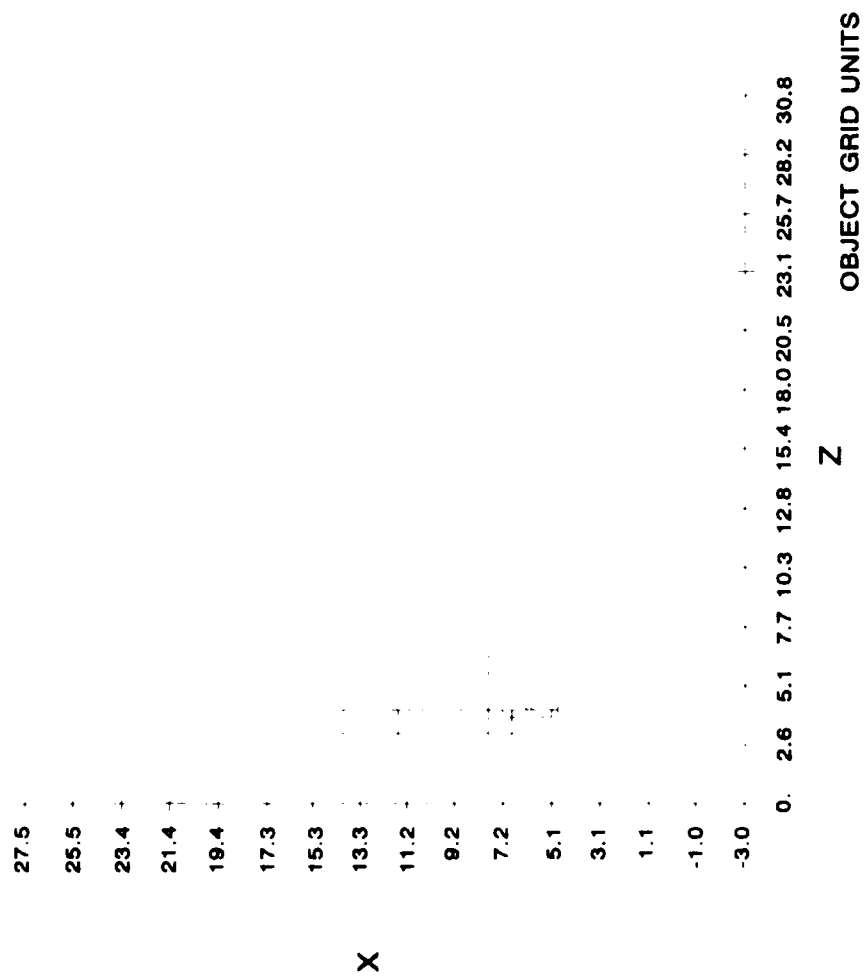


Figure 5(b). POLAR 2 model of disk and probe, side view.

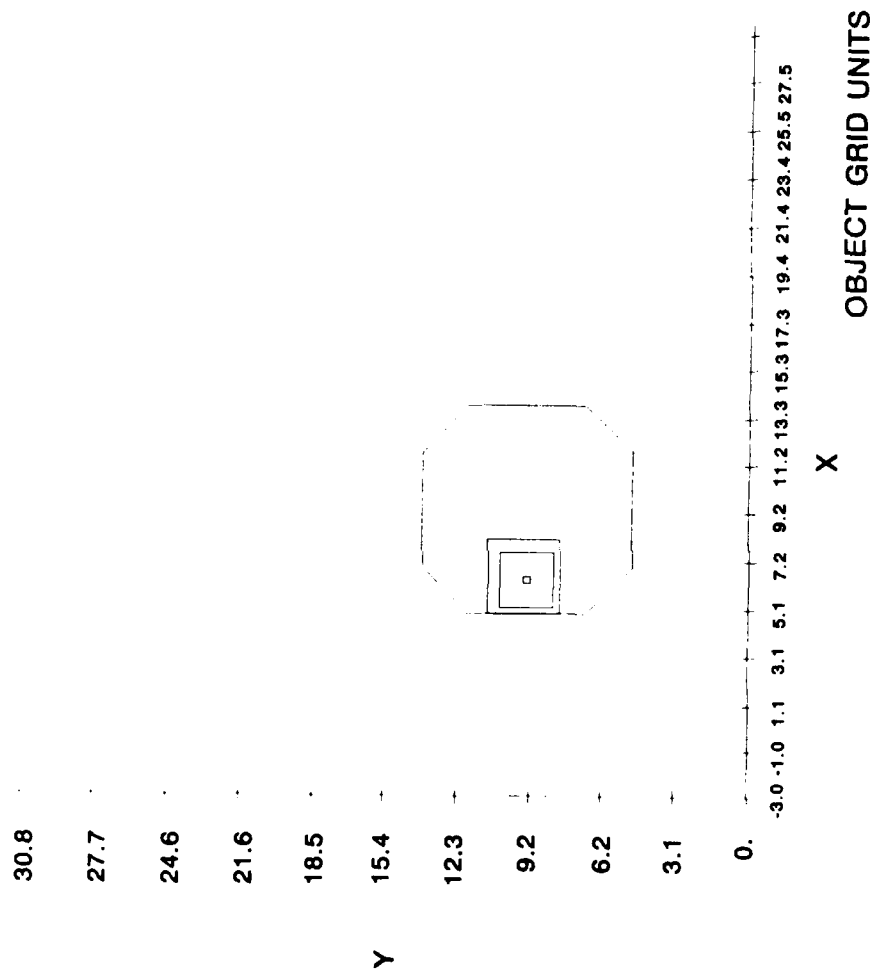


Figure 5(c). POLAR 2 model of disk and probe, back view.

- 1) upgrade the POLAR 2 code to enable it to calculate GI density.
- 2) use POLAR 1 to calculate the GI density and transport this data to POLAR 2.

The second option was chosen as it seemed to involve less coding, and it also enabled us to gain access to the POLAR continuation files, with an option to plot grid data on the IRIS 3D color workstation. The programs that were developed to do this data transfer are described in Appendix 1.

In POLAR, objects are held fixed and the gridding is adjusted to follow the flow direction. For off-axis flow, this entails the use of staggered grids, i.e. the grid nodes are successively offset as one goes downstream. This is shown in Figure 6, which gives the GI density at tilt angles 0, +20, and +40 degrees, as obtained from POLAR 1. The plots for the negative tilt angles would be the same, but inverted with respect to the x axis. This GI data was loaded into the POLAR 2 files, using the PATCHG module. POLAR 2 was then ready to start doing some physics, as is described in the next section.

3.0 POLAR 2 RESULTS FOR THE WAKE SHIELD MODEL

The POLAR 2 calculation of IV characteristics was generated in the following way. First, we did the setup procedure, as described in section 2, to configure the system for a specified tilt angle. A starting probe voltage was set and an initial calculation of potential was done using the GI approximation to density. Then, successive Vlasov (solve for density given the potentials) and Poisson (solve for potentials given the densities) cycles were carried out until a steady state was achieved. The probe potential was then increased to the next level and the run was continued until a new steady state was reached. This process was repeated until the entire IV curve was obtained. The configuration was then reset for the next tilt angle and the procedure repeated. The tilt angles were set to values of -40, -20, 0, +20, and +40 degrees, and the probe voltage was swept through -1, -3, -5, -7, and -9 KV. Two families of IV curves were generated, one for Debye length $D = 0.35$ cm and one at $D = 1.05$ cm.

Figure 7 shows the POLAR 2 solutions for grid potential at successive tilt angles, with probe voltage of -1 KV and -9 KV, for the case $D = 0.35$ cm. In the Figures, the plus signs represent the location of the equi-potential surface representing the sheath edge. The POLAR 2 Vlasov algorithm tracks inwards from this equi-potential in order to compute the sheath density and probe current. Note that the grid space is truncated at the downstream end, but this should not affect the currents, since the sheath edge contour is always far upstream, in the near wake of the disk.

The POLAR 2 results for ion current collection at $D = 0.35$ cm are shown in Figure 8. Here, the ion current (ma) is given as a function of probe voltage (KV), with the tilt angle as parameter. A positive tilt angle represents a rotation of the near edge of the disk towards the ram direction, and a negative angle rotates away from the ram as indicated in Figure 2. It can be seen in Figure 8 that, excluding the -40 degree case, the current tends to increase monotonically as the tilt angle increases. This is to be expected, since the rotation towards positive tilt angles increases the exposure of the near edge of the disk to the ram flux. The one exception to this trend is the case of -40 degrees, where there is a significant current enhancement, especially at the higher probe voltages. This effect is more apparent in Figure 9, which is a re-plot of the data in Figure 8, but now with tilt angle as independent variable and each curve representing a different probe voltage. In Figure 9, the current enhancement at a large negative tilt angle

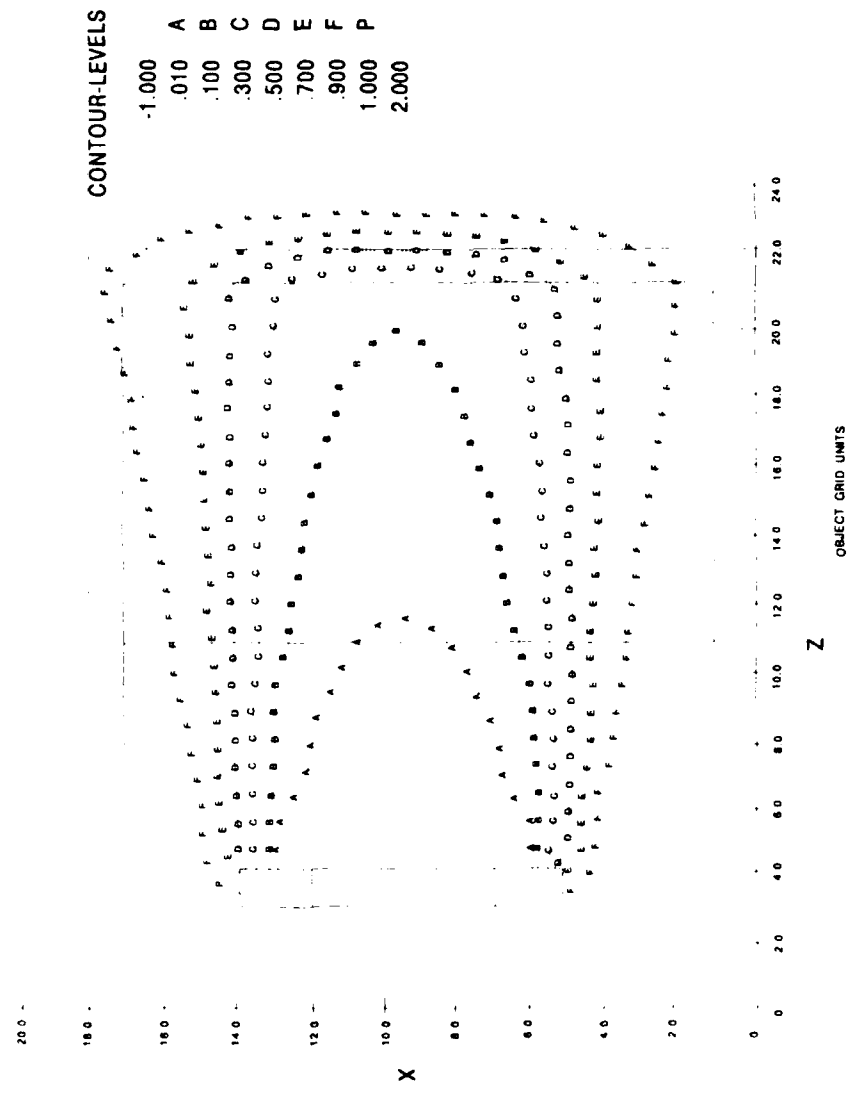


Figure 6(a). POLAR 1 geometrical ions, tilt = 0 degrees.

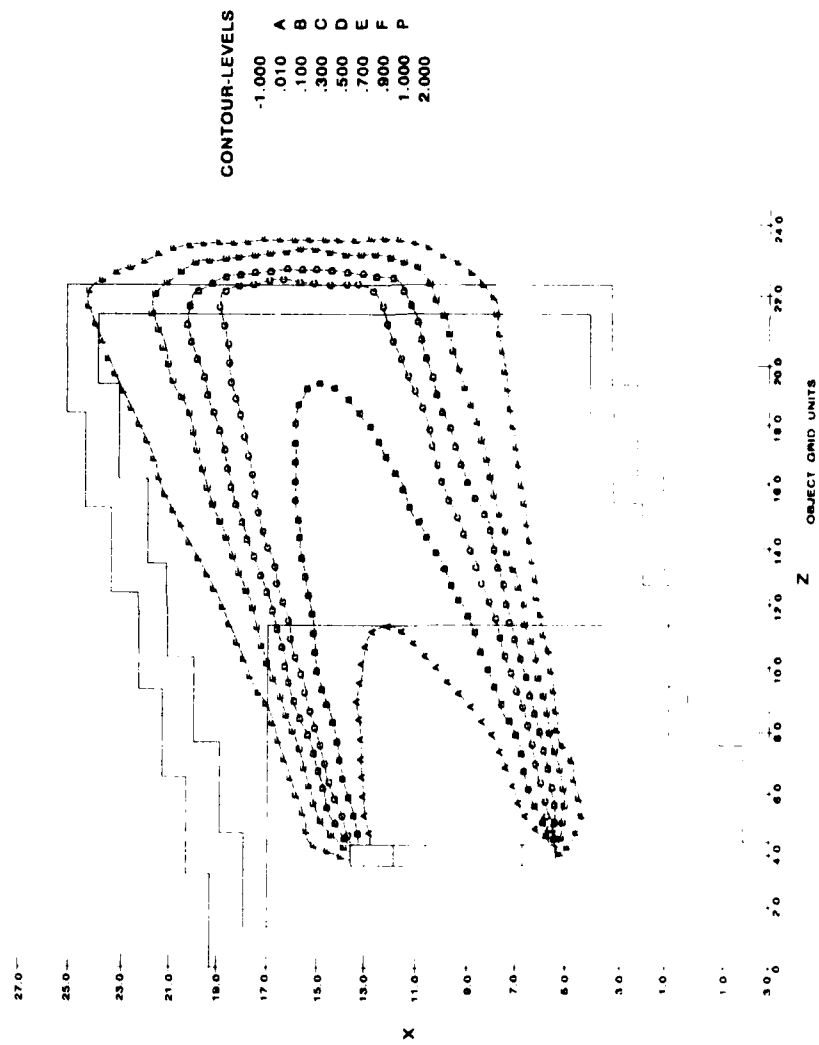


Figure 6(b). POLAR I geometrical ions, tilt = +20 degrees.

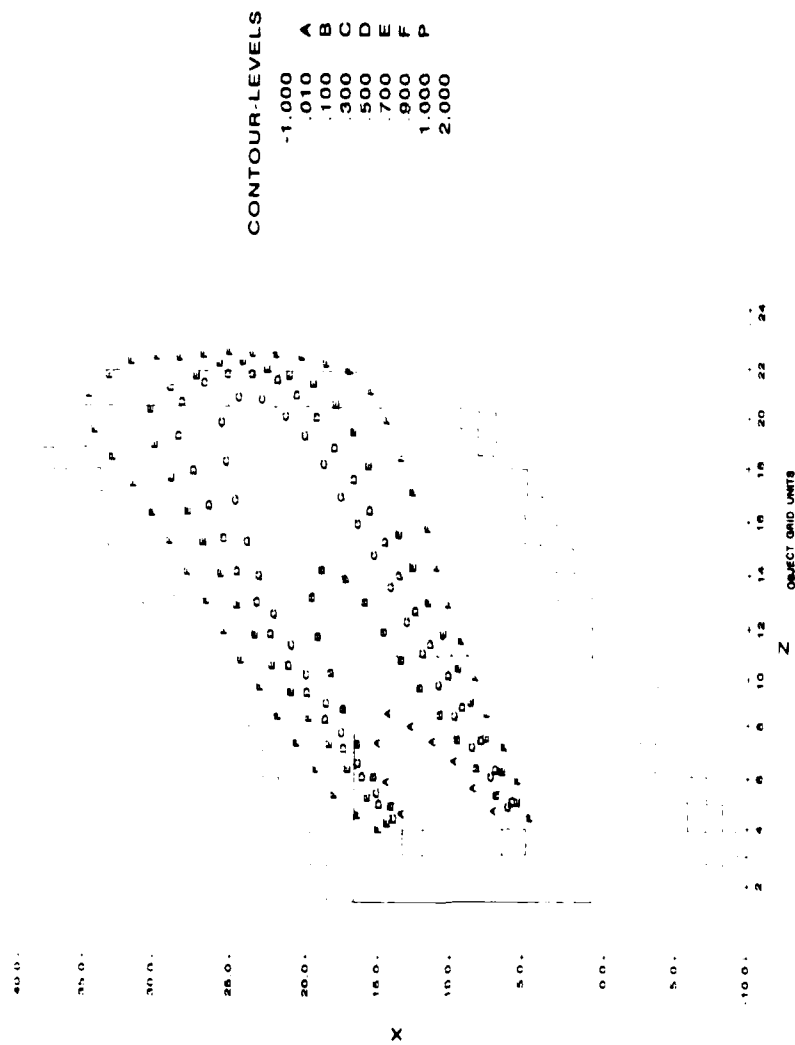


Figure 6(c). POLAR 1 geometrical ions, tilt = +40 degrees.

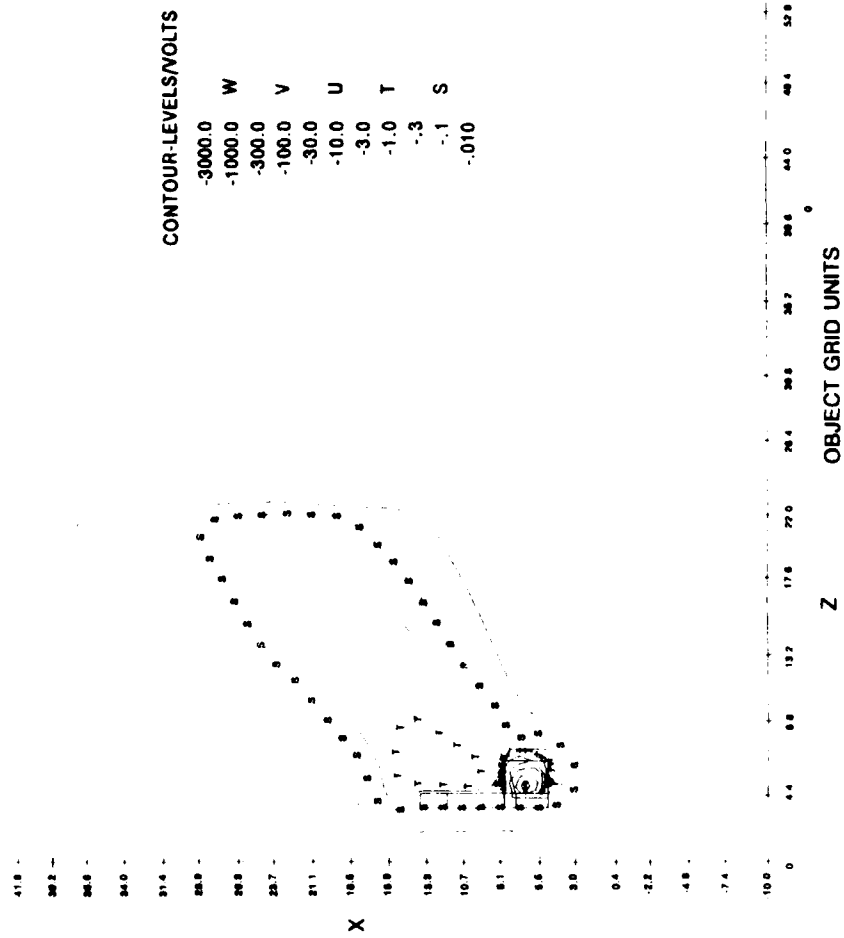


Figure 7(a). POLAR 2 potential contours; probe at -1 KV, D = 0.35, tilt = +40 degrees.

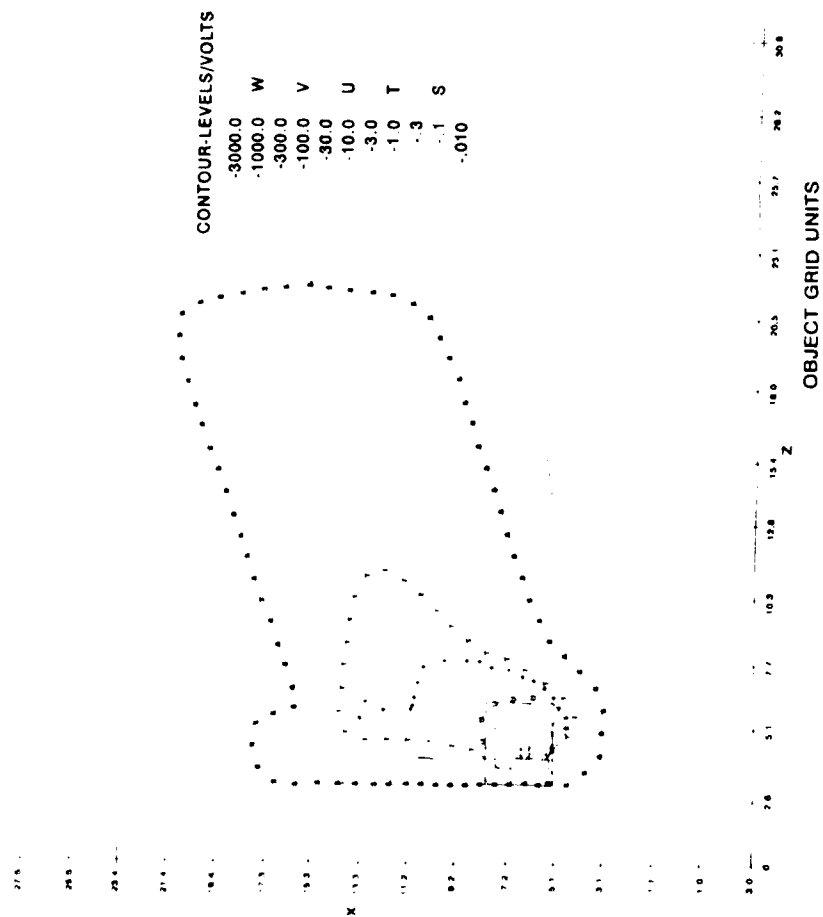


Figure 7(b). POLAR 2 potential contours; probe at -1 KV, D = 0.35, tilt = +20 degrees.

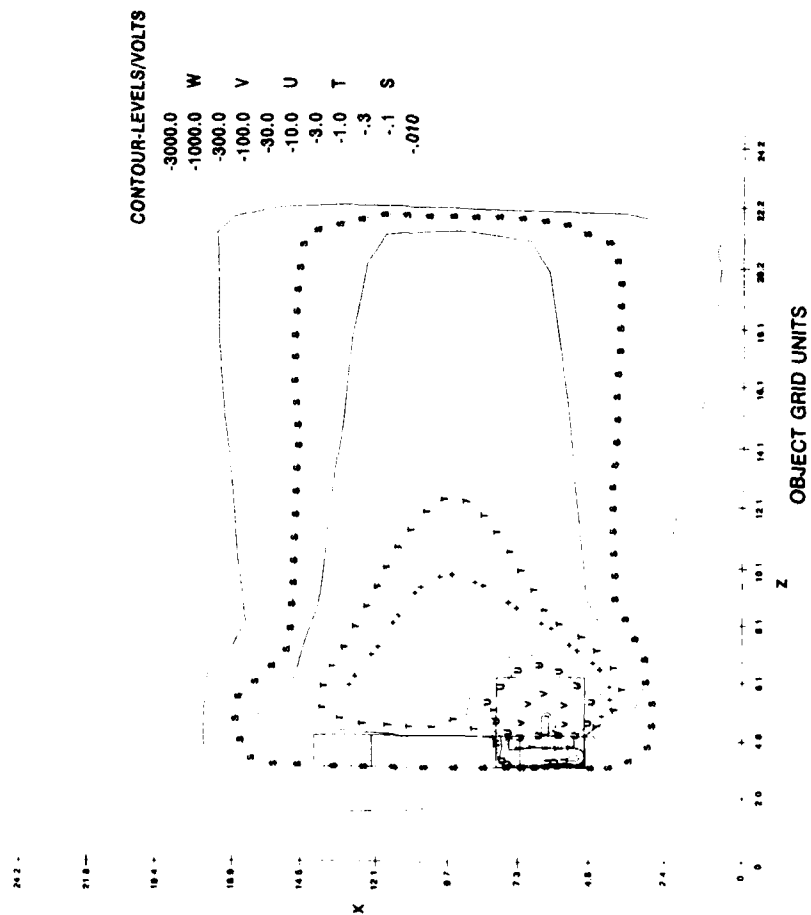


Figure 7(c). POLAR 2 potential contours; probe at -1 KV, D = 0.35, tilt = 0 degrees.

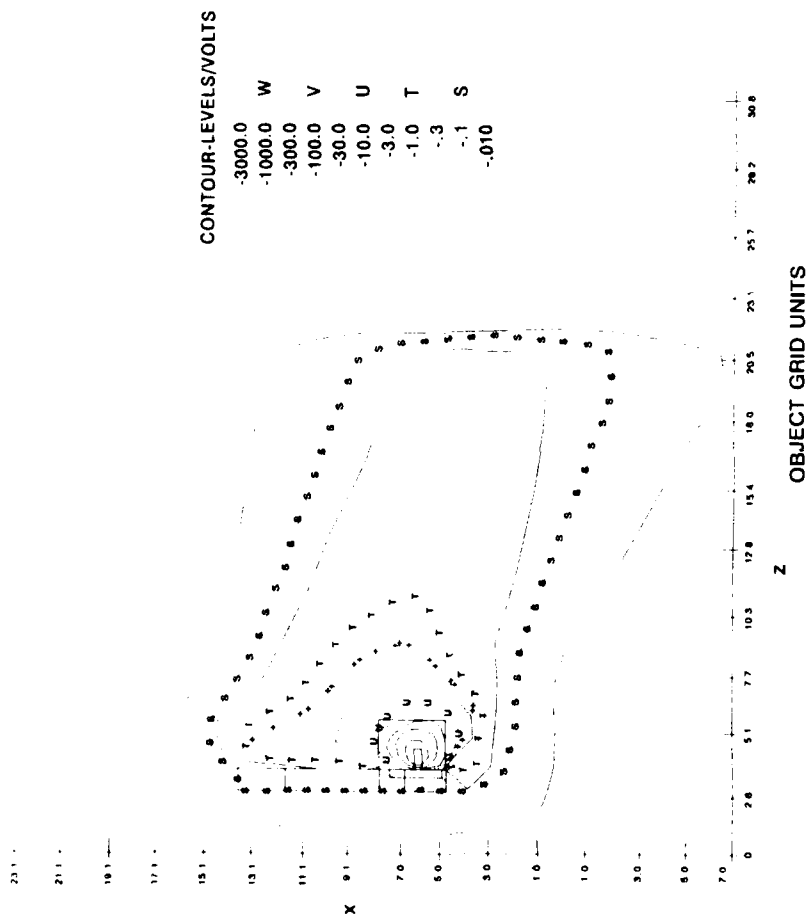


Figure 7(d). POLAR 2 potential contours; probe at -1 KV, $D = 0.35$, tilt = -20 degrees.

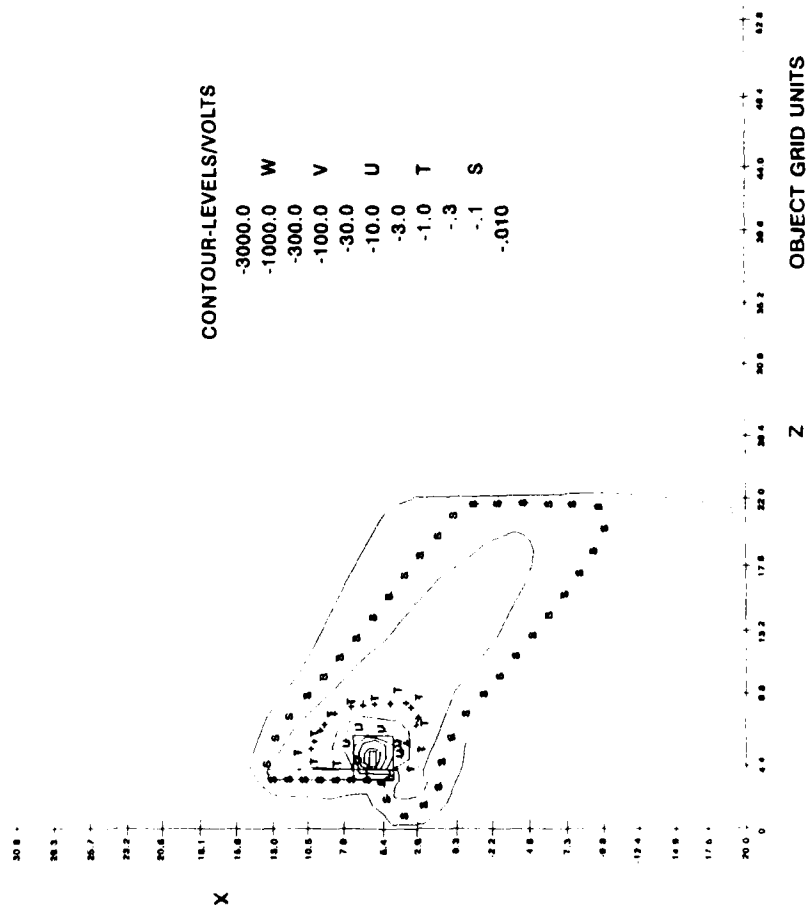


Figure 7(e) POLAR 2 potential contours; probe at -1 KV, D = 0.35, tilt = -40 degrees.

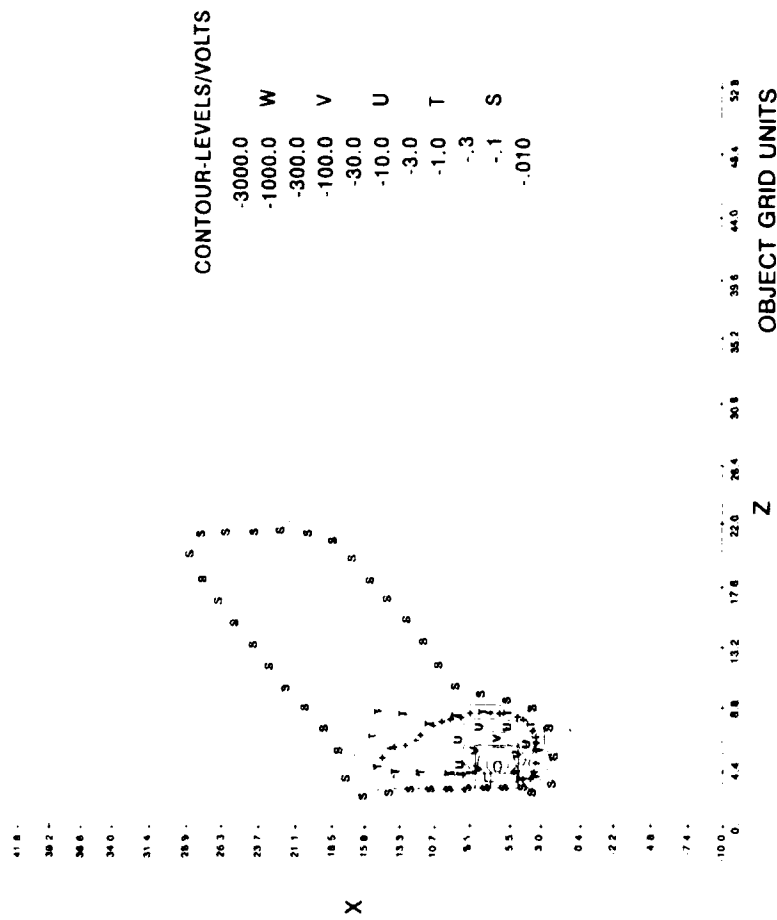


Figure 7(f). POLAR 2 potential contours; probe at .9 KV, $D = 0.35$, tilt = +40 degrees.

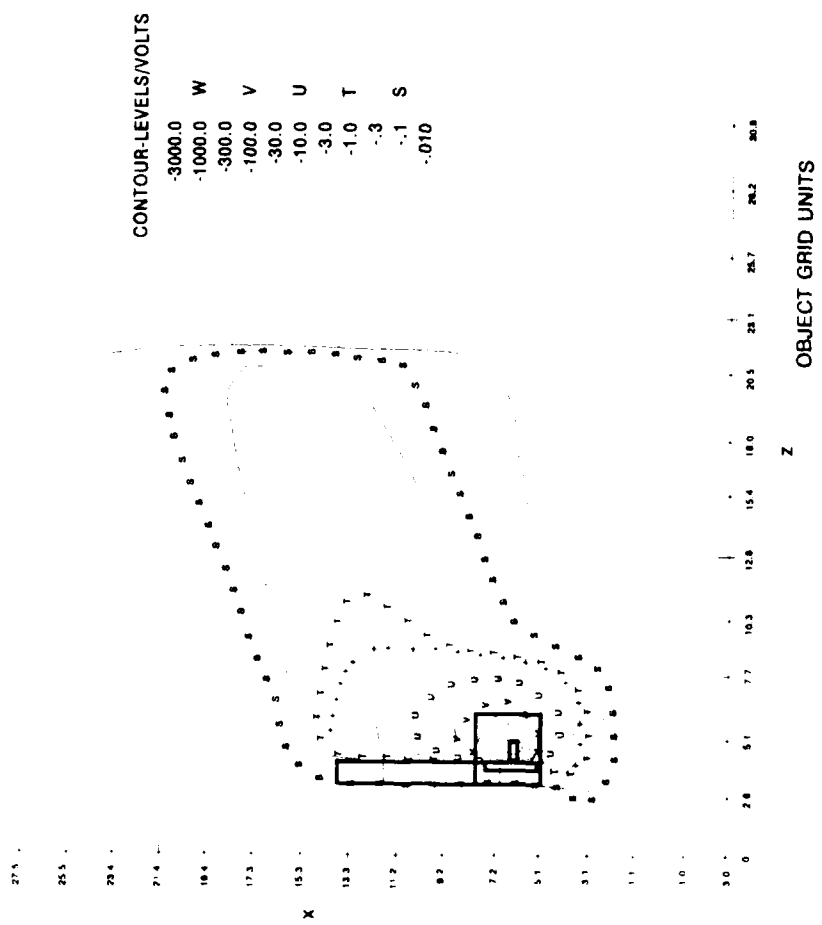


Figure 7(g). POLAR 2 potential contours; probe at -9 KV, D = 0.35, tilt = +20 degrees.

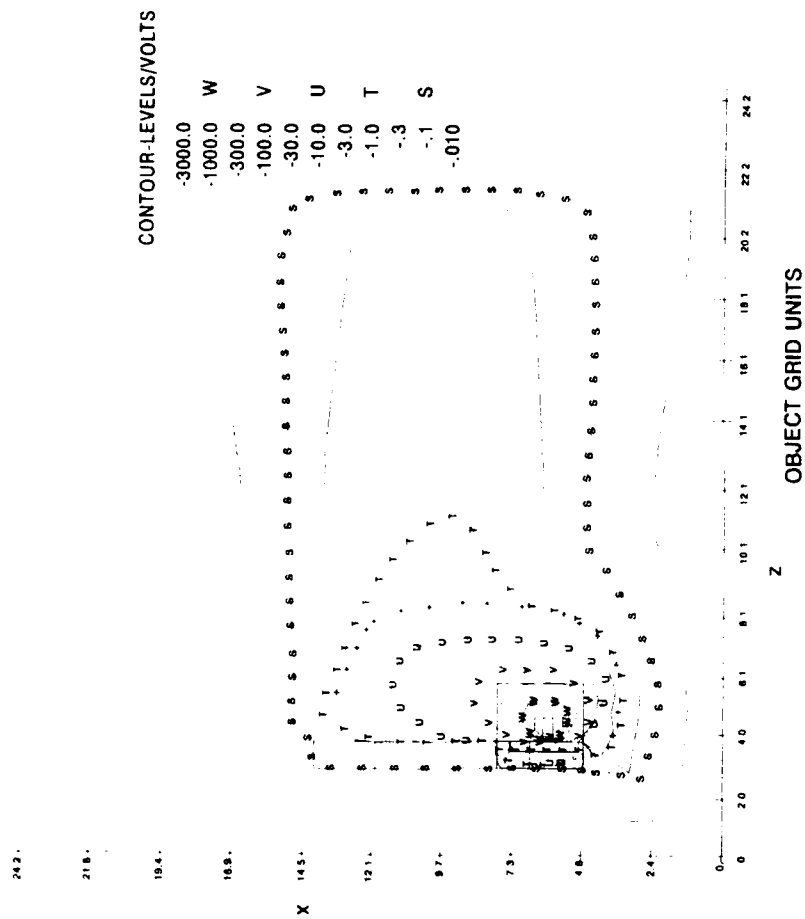


Figure 7(h). POLAR 2 potential contours; probe at -9 KV, D = 0.35, tilt = 0 degrees.

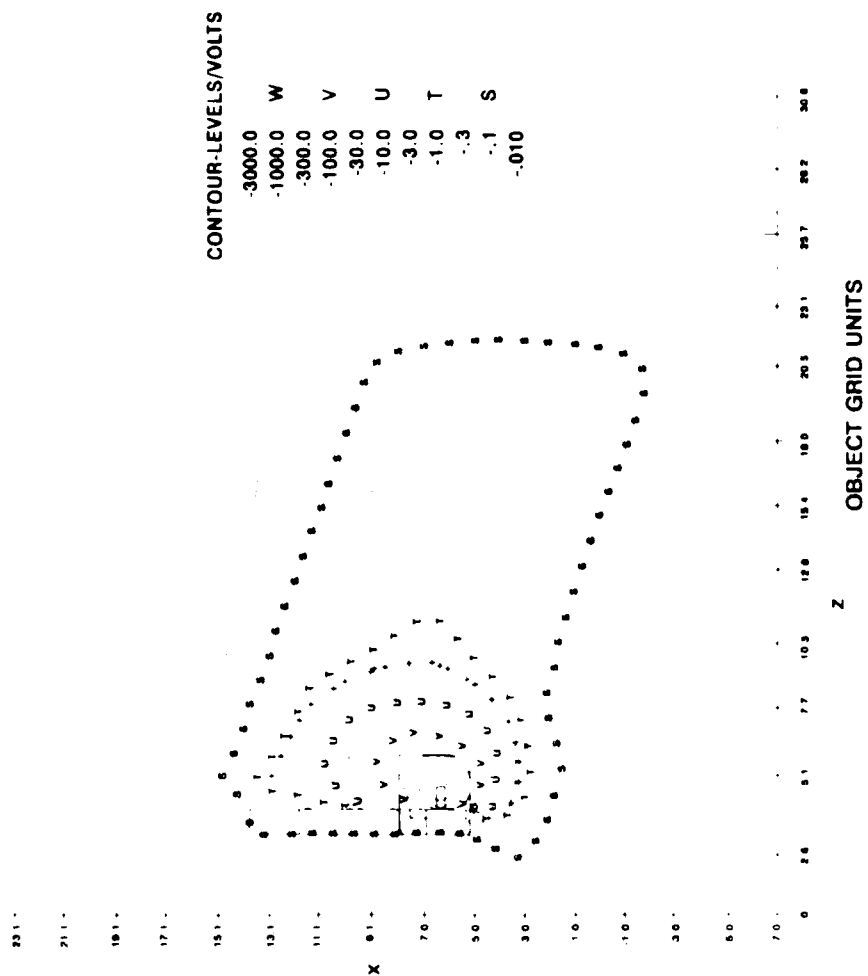


Figure 7(i). POLAR 2 potential contours; probe at -9 KV, D = 0.35, tilt = -20 degrees.

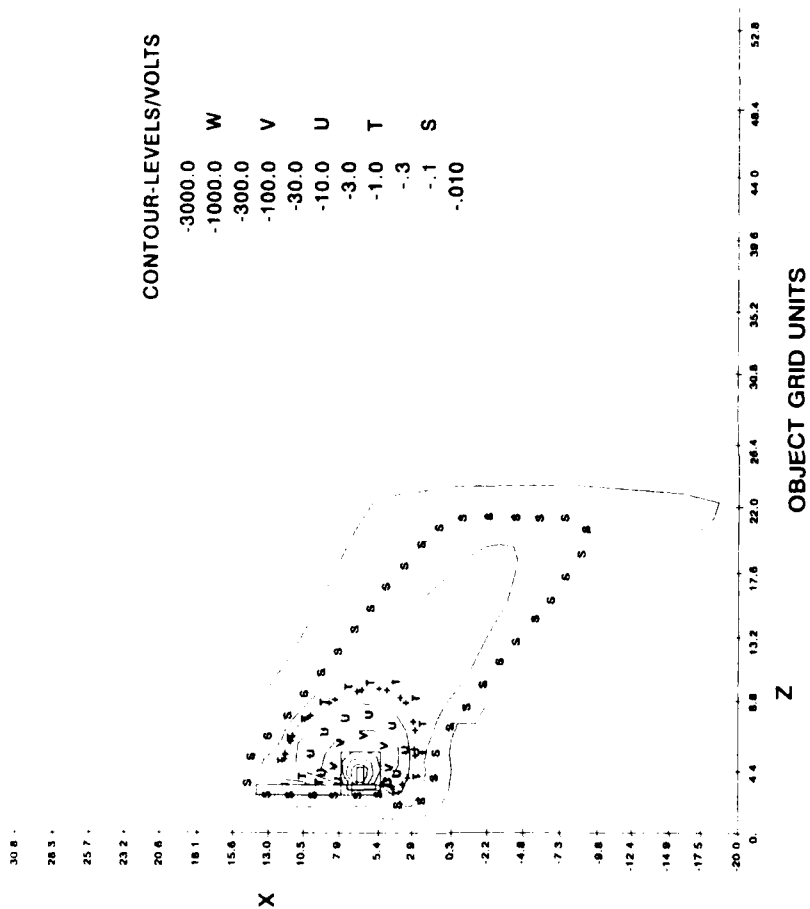


Figure 7(j). POLAR 2 potential contours; probe at -9 KV, D = 0.35, tilt = -40 degrees.

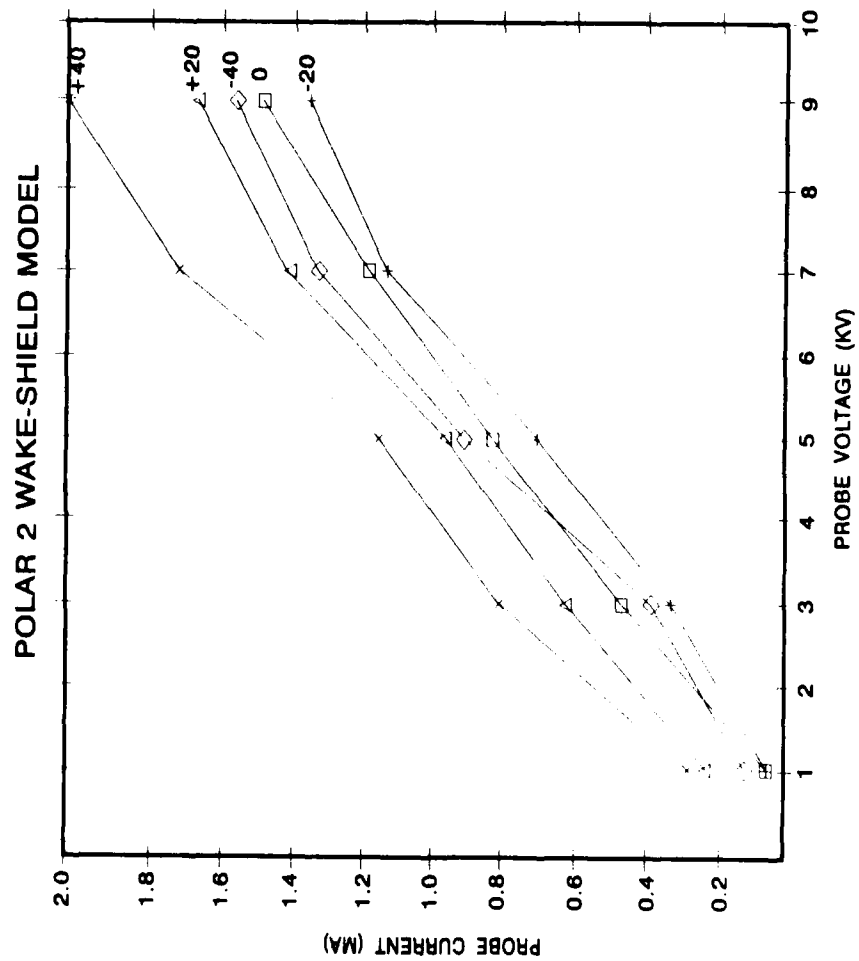


Figure 8. Current-Voltage characteristics for $D = 0.35$.

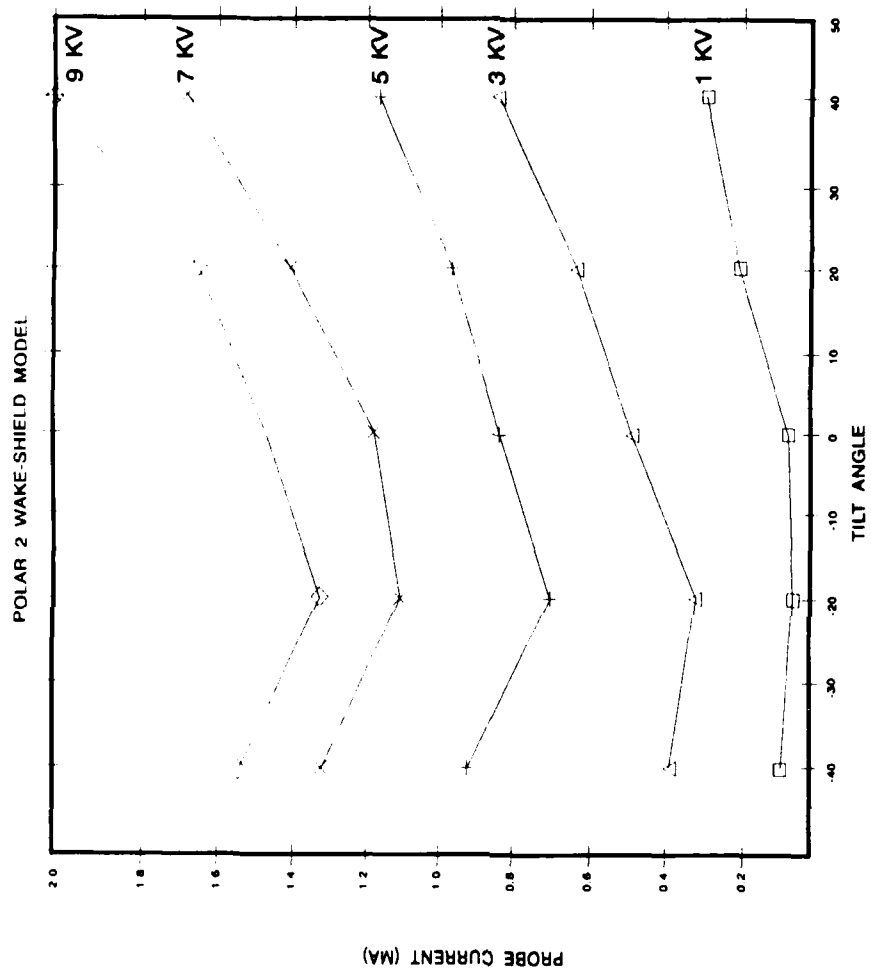


Figure 9. Probe currents versus tilt, $D = 0.35$.

can be seen clearly for all voltages greater than 1 KV. We can understand this current enhancement as being due to 'cross-over' trajectories. That is, when the negative tilt angle gets large enough and the electric field of the probe gets strong enough, the particles crossing the far edge of the disk can enter the sheath and be captured by the probe. These trajectories carry a large current since they are directly in line with the ram flux. To illustrate this effect, we show in Figure 10 some sample trajectories at probe voltage -9 KV. The Figure depicts trajectories at zero, +40, and -40 degrees tilt angles. The trajectories are colored according to the value of the local potential at each time step. The potentials range from zero (red) to the probe potential (blue). One can see that, at zero tilt, the current is collected mainly from the near disk edge. At +40 degrees this is also true, and current collection goes up, due to the increased exposure to the ram flux. At -40 degrees the current collected from the near edge decreases, due to the decreased exposure to the ram, but there is now a second source of current at the far edge, from the cross-over trajectories.

We now consider the case where the Debye length is increased by a factor of 3 (equivalent to the ambient density being scaled by $1/9$) to $D = 1.05$ cm. Figure 11 shows the POLAR 2 solutions for potentials at tilt angles -40, 0, and +40. These plots can be compared to Figures 7(a), (c), and (e) above. The main difference between the solutions at $D = 0.35$ and $D = 1.05$ cm is that sheath size is larger for the latter case. The increase of sheath size with increasing Debye length is a general phenomena which occurs because the electric field can penetrate more easily into a less dense plasma.

Figures 12 and 13 show current versus probe voltage and tilt angle, in the same format as for Figures 8 and 9. It can be seen that the magnitude of the current is now much smaller, and this can be attributed mainly to reduced ram flux (longer Debye length corresponds to smaller ambient density and hence to smaller ram flux). The decrease in current is less than the density scaling factor ($1/9$) because the relatively larger sheath collects more current than the smaller sheath.

The POLAR 2 code model also gives information on the distribution of current over the outward facing probe surfaces. These surface elements have been numbered 1 to 13, starting at the bottom of the probe and working up, as shown in Figure 14. The percentage of the total current, at each probe voltage, is plotted versus cell number in Figure 15 for the $D = 0.35$ case and in Figure 16 for $D = 1.05$. In the Figures, the different symbols represent the different probe voltages, with the same symbols for voltage as was used in Figure 9. By symmetry, we expect that currents at the +y and -y sides of the probe (cells 1 and 4, 5 and 8, 9 and 12) should be almost equal, and this gives a check on the accuracy of the solutions. A comparison of the currents on the +x side (cells 2, 6, and 10) versus the -x currents (cells 3, 7, and 11) shows that current tends to be preferentially collected on the +x side, which is the side facing away from the near edge. Thus, the tracks tend to curl around the probe and hit the back surfaces, rather than impinging directly on the front side. Another trend that is apparent is that, for $D = 0.35$, more current tends to fall on the upper surfaces than near the base of the probe, notably at large tilt angles. This tendency is not apparent for the $D = 1.05$ case, where the current distribution tends to be flatter and there is reduced intensity on the top of the probe.

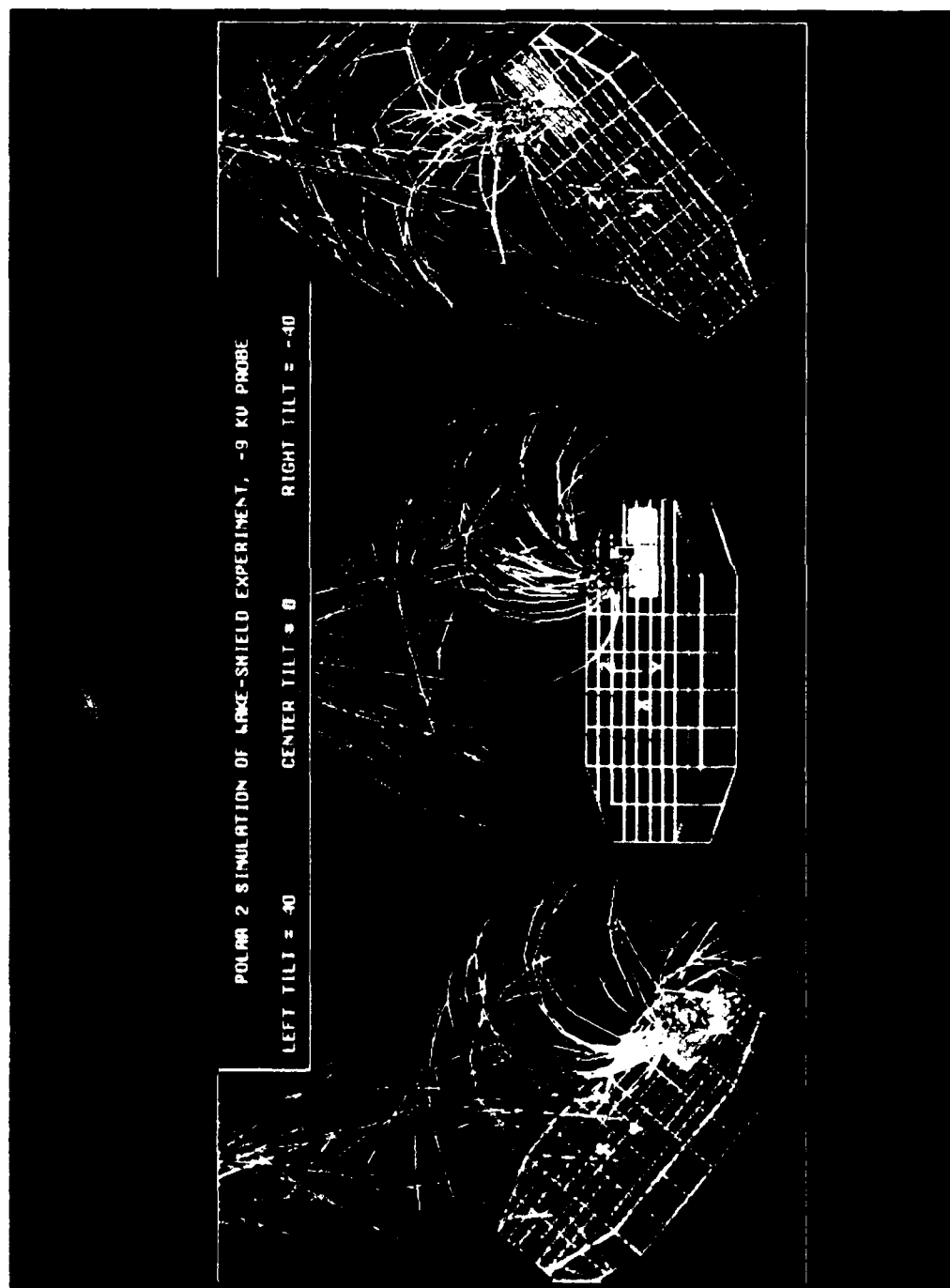


Figure 10. POLAR 2 Data Lines D - 0.35

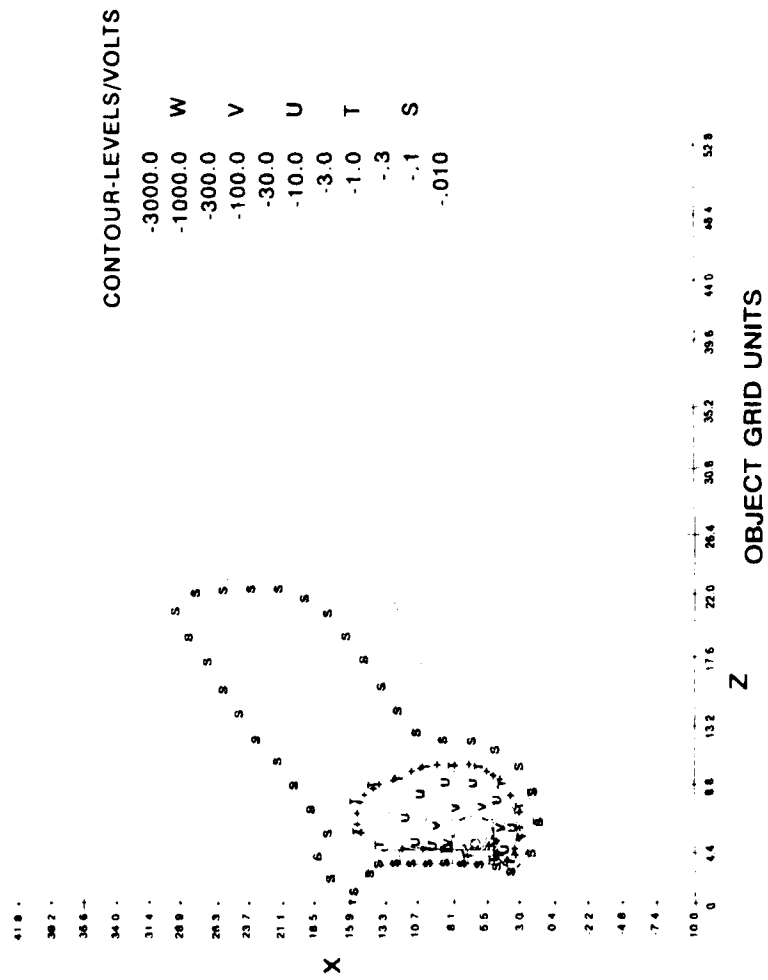


Figure 11(a). POLAR 2 potential contours; probe at -9 KV, D = 1.05, tilt = +40 degrees.

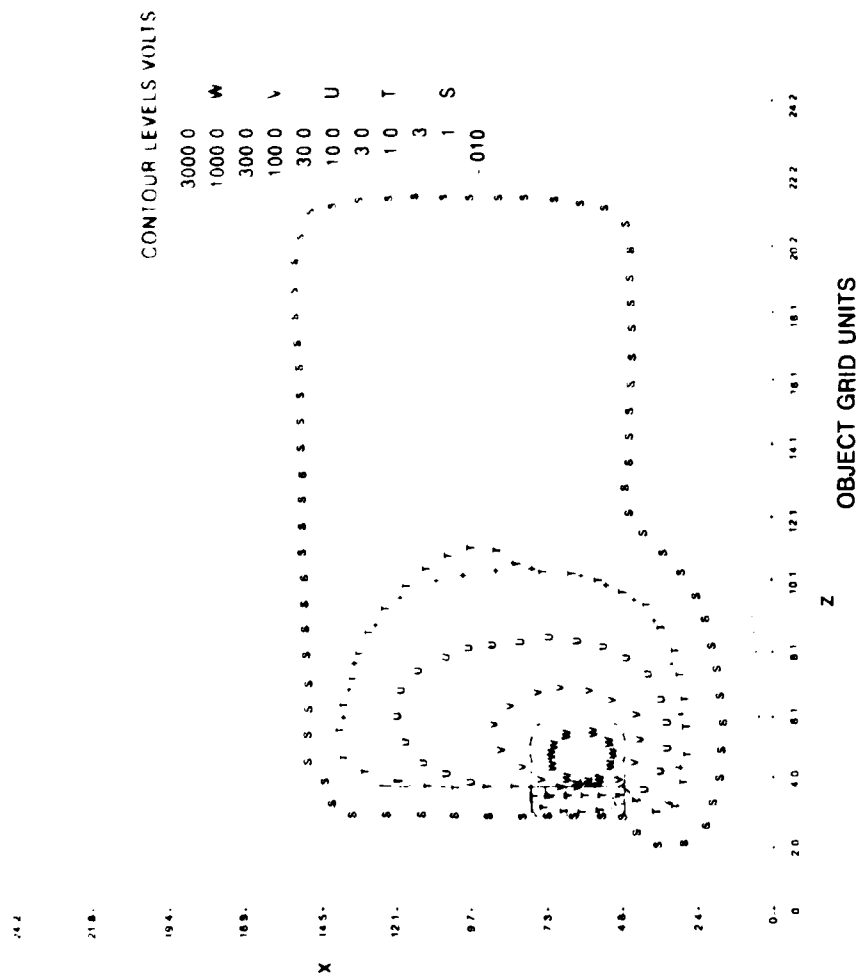


Figure 11(h). POLAR 2 potential contours; probe at -9 KV, D = 1.05, tilt = 0 degrees.

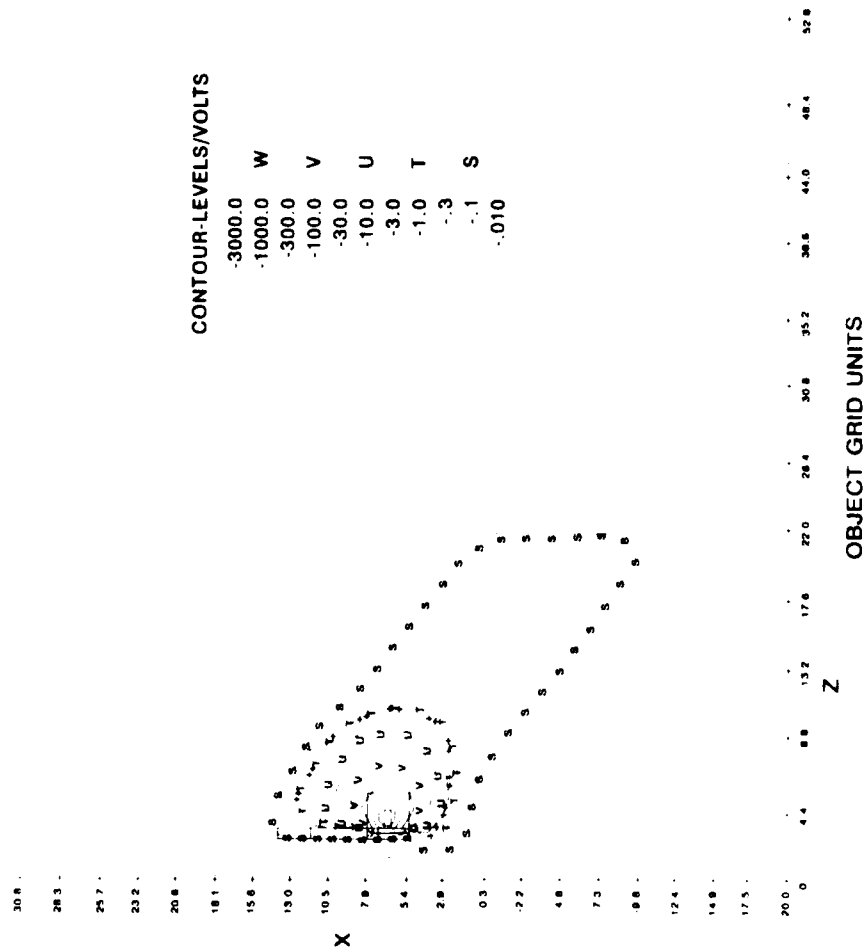


Figure 11(c) POLAR 2 potential contours; probe at -9 KV, D = 1.05, tilt = -40 degrees.

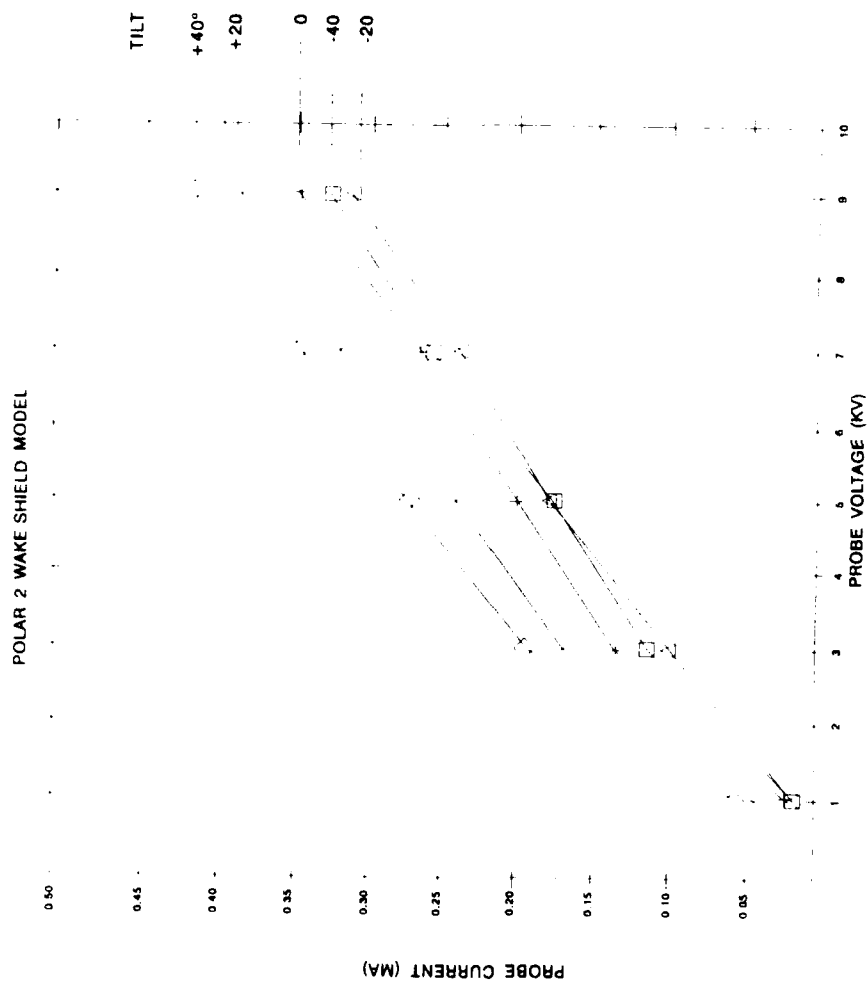


Figure 12. Current-Voltage characteristics for $D = 1.05$.

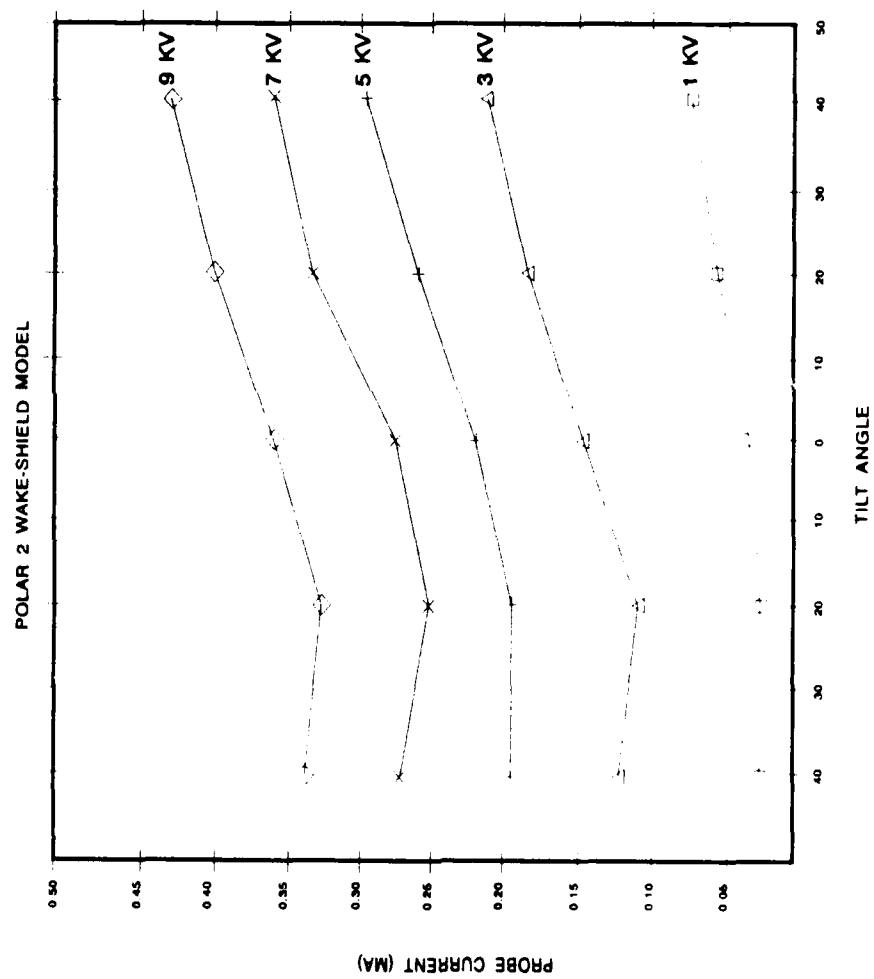
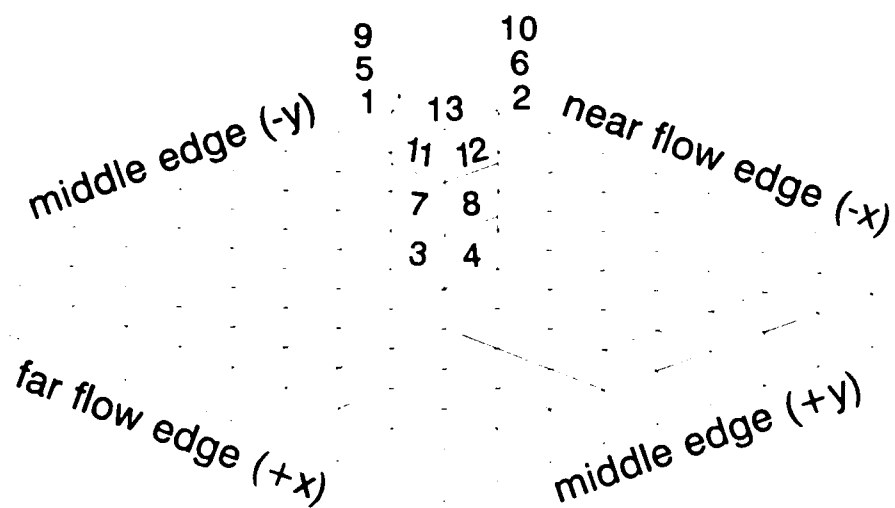


Figure 13. Probe currents versus tilt, $D = 1.05$.



z

z is plasma flow
direction

x

y

Figure 14. Surface cell numbers on the probe.

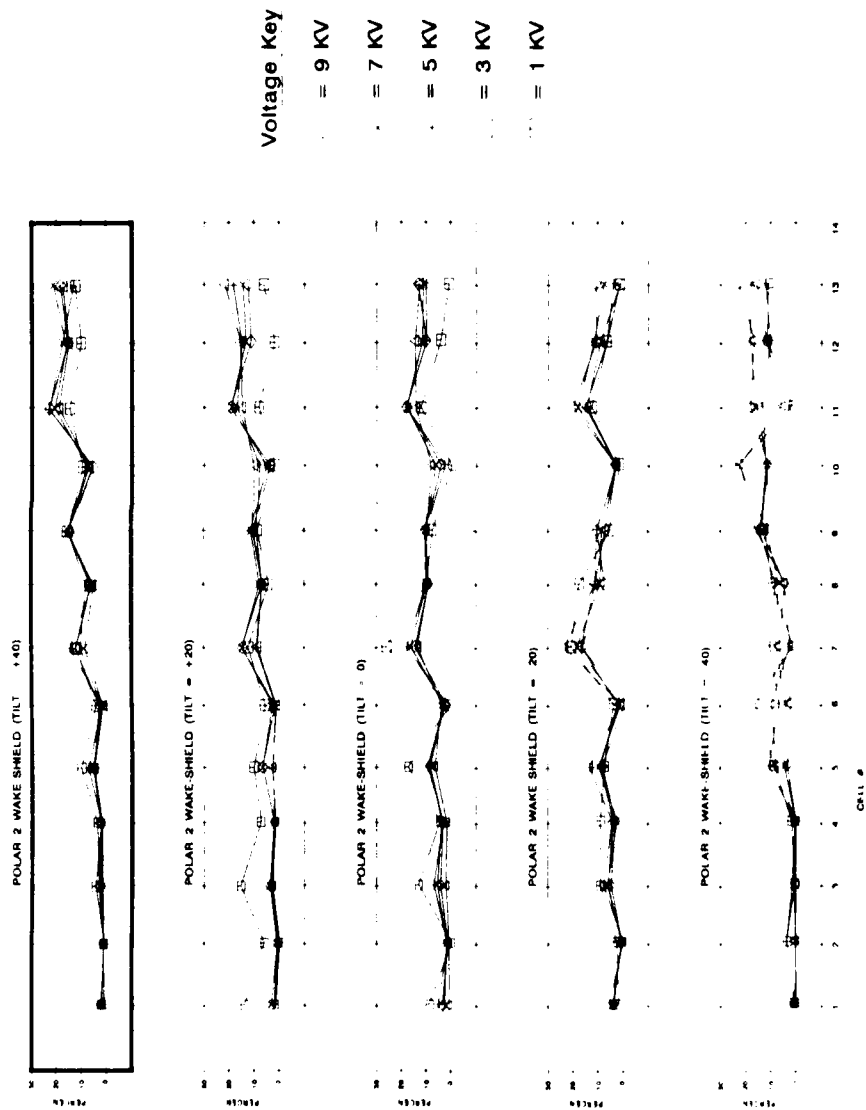


Figure 15. Surface cell currents, $D = 0.35$.

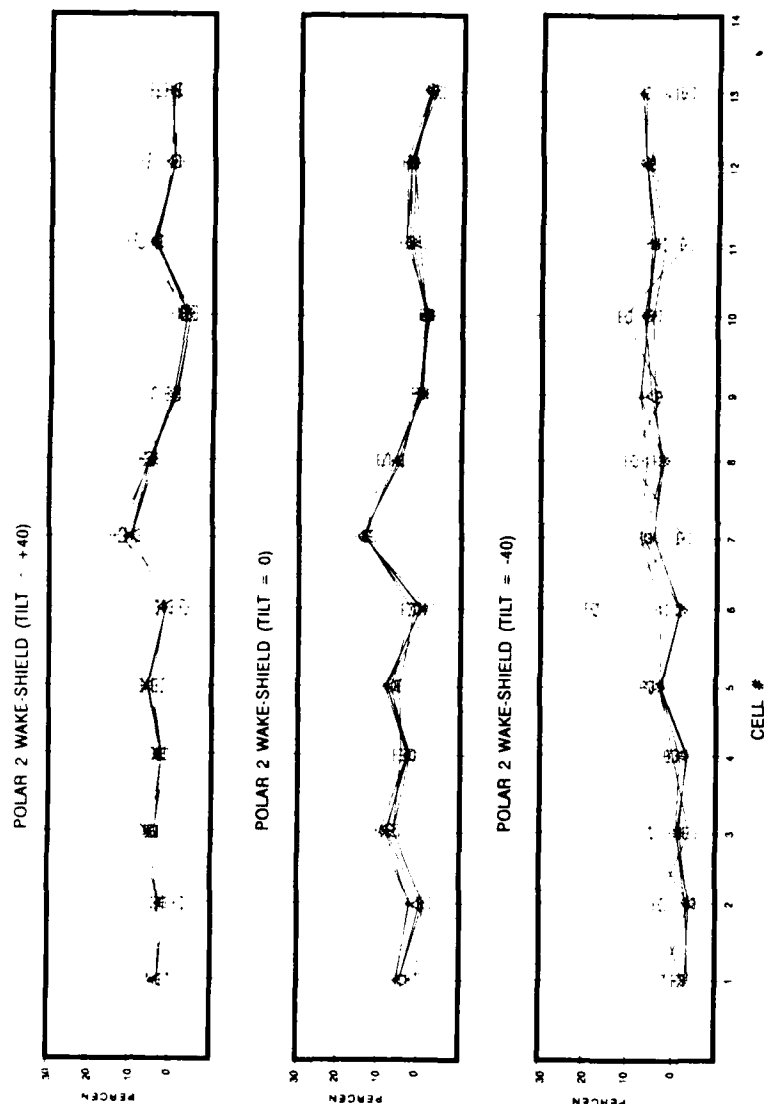


Figure 16. Surface cell currents, $D = 1.05$.

4.0 CONCLUSIONS

We have run POLAR 2 to investigate the IV characteristic of a charged probe in the shielding wake of an uncharged disk in a plasma environment set to represent typical shuttle orbit conditions. The probe was positioned approximately 0.4 meters from the near edge of a 3 meter diameter front disk. A tilt angle of the front disk, away from the nominal orientation perpendicular to the plasma flow direction, was varied from -40 degrees to +40 degrees in steps of 20 degrees. The probe voltages went from negative 1 KV to negative 9 KV in steps of -2 KV. Two plasma Debye lengths were considered, $D = 0.35$ cm and $D = 1.05$ cm. The POLAR 2 predictions for this wake shield model are:

- 1) The shielded probe should collect up to 2 ma of current at $D = 0.35$ (density $9 \times 10^{11} \text{M}^{-3}$, temperature 0.2eV), depending on the tilt angle, at the highest voltage of -9 KV. At lower voltages, the current drops, approximately linearly, to below 0.5 ma at -1 KV.
- 2) At $D = 1.05$ the maximum current collection is reduced to less than 0.5 ma. The dependence on tilt angle is qualitatively the same.
- 3) The current collection should increase with rotations towards the ram (positive tilt angles).
- 4) For rotations towards negative tilt angles, the current first decreases and then picks up again as the tracks which cross over from the far side of the disk start to be collected. At $D = 0.35$ the turn-around point, for minimum probe current, occurs between -20 and -40 degrees. At $D = 1.05$ the effect is more gradual and some cross-over tracks occur even at zero tilt angle.
- 5) Except for the cases with large negative tilt angle, more current is collected on the side of the probe away from the near edge of the disk than on the side facing the near edge.
- 6) At $D = 0.35$, the current distribution over the probe favors more current at the top than near the base. At $D = 1.05$ the current distribution is flatter and tends to be reduced at the top of the probe.

The maximum currents given here give upper limits, since the design limit for the wake shield probe is -5 KV and only the middle band and the top of the probe will be conducting. Based on the IV curves shown in Figure 8, we would expect about 1 ma of current to impinge on the probe at -5 KV.

REFERENCES

- Chan, C. J. Browning, S. Meassick, M. A. Morgan, D. L. Cooke, C. L. Enloe, and M. F. Tautz, "Current Collection in a Spacecraft Wake; Laboratory and Computer Simulations", PL-TR-93-2027(II), 1993. ADA263216
- Cooke, D. L., M. S. Gussenhoven, D. A. Hardy, M. F. Tautz, I. Katz, G. Jongeward, J. L. Lilley, "Polar Code Simulation of DMSP Satellite Auroral Charging", PL-TR-93-2027(I), 1993. ADA263215
- Jongeward, G. A., M. J. Mandell, J. Lilley, I. Katz, "POLAR 2.0 Validation and Preflight SPEAR I Calculations", AFGL-TR-88-0056, 1988. ADA201094
- Katz, I., G. A. Jongeward, V. A. Davis, M. J. Mandell, R. A. Kuharski, J. R. Lilley, W. J. Raitt, D. L. Cooke, R. B. Torbert, G. A. Larson, and D. Rau, "Structure of the Bipolar Plasma Sheath Generated by SPEAR I", *J Geophys Res*, **94**, (A2), 1450-1458, February 1, 1989.
- Lilley, J. L., D. Cooke, G. Jongeward, and I. Katz, "POLAR User's Manual", GL-TR-89-0307, 1989, ADA232103.

APPENDIX. POLAR 2 PROGRAMMING NOTES

In order to move the geometrical ions (GI) from POLAR 1 to POLAR 2, a whole new module associated with PATCHG (see Figure 2) was written. This module is comprised of four separate programs:

- getp1 - this program reads POLAR 1 files fort.11,19 and writes a MSIO file called fort.26. The MSIO file has a general format so that potentials, etc. can be written, as well as the GI.
- patg - this program reads file fort.26 and puts the GI into the POLAR 2 files fort.11,19. It is assumed that the POLAR 1 and POLAR 2 grids are compatible, i.e the disk object is the same for both, and the ion mach number is constant, so that the staggered grid nodes will line up.
- getp2 - this program reads POLAR 2 files fort.11,19 and writes a MSIO file called fort.27. This program is needed because POLAR 2 does not plot any grid variables except potentials. The fort.27 file (and also fort.26) can be read by the IRMA plotting program on the IRIS 3030 work station to produce 3 dimensional color plots of the potentials, ion densities, and the GI.
- readb - this is a check up program used to read back either the fort.26 or fort.27 MSIO file and write out a grid slice in SUATEK format. In this form, the data can be plotted with SUATEK (for 1D profiles) or MACHCON (for 2D contours).

These routines provide an adequate set of tools for handling POLAR 2 data files and to interface to our existing plotting programs IRMA, SUATEK, and MACHCON. Each program has its own input stream and output switches.

The notes below list miscellaneous changes made to POLAR 2 in the course of this study. The major programming change was to routine dblchk.f. This routine was not implemented for multi-grids and had to be developed from the POLAR 1 prototype.

| | | |
|-------------|---------------------|--|
| dens module | / dblchk.f | implemented multi-grid version |
| | / optin.f, sthcal.f | implemented nosthcal keyword for selectively disabling grid sheath particles |
| | / optdef.f | changed default ipcnt = 5 from 3. |
| pot module | / potfix.f | commented out unwanted initialization |
| | / qscrn2.f | fixed stability parameter dqreal sign bug |

| | | |
|--------|------------------------|--|
| pollib | / efield.f | force stppsh to do boundary checking in the inner grids so vertio will not crash |
| | / getgrd.f | skip the search for inner grids when on a boundary, otherwise ipufad crashes |
| shontl | / many | added new keywords for track display |
| | | WGTCUT 1 0.1 10. cut tracks on weights from 0.1 to 10. |
| | | TR3D = 0 tracks are colored by weights |
| | | = 1 tracks are colored by potentials |
| | | FILTER = n gives track reduction modulo n |
| | | NOSTHCAL = m skips particle tracking from grid m used for testing |
| patchv | / patchv.f
mksgrd.f | added error level input to bypass tolerable errors |

Note: when patg is executed, this is counted as the first pass of nterak, and as such treats the inputs slightly differently. Thus, it is important to keep the patg input files consistant with the actual run parameters used later, e.g. it was found that if the TEMP parameter is different, it will crash the run.